Biophysical Chemistry, 39 (1991) 153–159

BIOCHE 01535

The effect of point mutations on energy profiles in a model of the nicotinic acetylcholine receptor (AChR) channel

S. Furois-Corbin and A. Pullman

Laboratoire de Biochimie Théorique, Institut de Biologie Physico-Chimique, 13, rue Pierre et Marie Curie, 75005 Paris, France

Received 5 June 1990
Accepted 5 August 1990

Acetylcholine receptor channel; MII-helix model; Na^+ energy profile; Point mutation

Energy profiles are calculated, using energy optimization computations, for a sodium cation in the AChR channel and four of its mutants, αE241D, βE247Q, δE255Q and αE241Q, using the model developed previously. The relative energy location of the calculated profiles confirms and specifies the role of each of the Glu residues found in the anionic ring at the bottom of the MII helices. The structural analysis of the results allows the understanding of the differences observed in the conductances for the wild-type and mutant αE241D, or for the mutants βE247Q and δE255Q in spite of the identity of the global charge of both channels in each couple. The striking correlation observed between the average relative energy location of the profiles and the conductance data appears to provide confirmation of the essential structural features adopted in the model, in particular the inclusion of the Glu(Gln in γ)-Lys residues in the α-helical stretch of the MII helices and the overall location of the internal residues.

1. Introduction

Using the presently available structural knowledge on the nicotinic acetylcholine receptor (AChR), supplemented by conditions derived from labelling experiments with non-competitive blockers (NCB) [1–4], we have recently developed [5–8] a model of the inner wall of the transmembrane

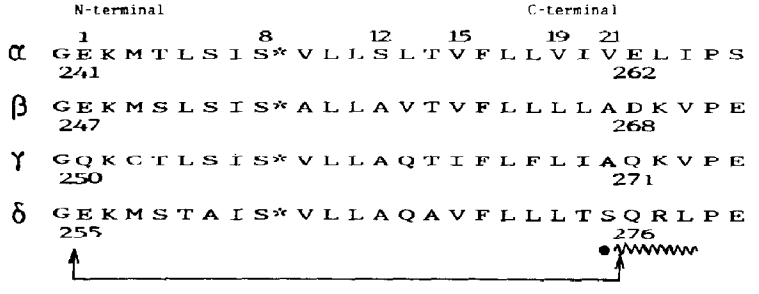

Fig. 1. Aligned sequences (standard numbering as indicated) of the MII hydrophobic segments of *Torpedo marmorata* and *T. californica* AChR with the limits (within the arrows) adopted in refs 5, 6 and 8; * homologous serines labelled by ^{3}[H]CPZ and ^{3}[H]TPMP; (∧∧∧) region of probable bend. For practical reasons a simplified numbering scheme is indicated on the top line.

Correspondence address: A. Pullman, Laboratoire de Biochimie Théorique, Institut de Biologie Physico-Chimique, 13, rue Pierre et Marie Curie, 75005 Paris, France.

channel of the receptor, in which the five MII helices (see the sequences in fig. 1) are pentagonally arranged around the central pit in the disposition of fig. 2: adopting the assumption [2] that the homologous serines labelled by the NCBs face the center of the pore, it was first shown [5] that, in order for the NCBs to block the channel at or in the neighborhood of these residues, consecutive MII helices must be laterally in contact at this level rather than separated by another helix, a feature which allows the determination [6] of the minimal distance in this region. It was further shown that, in order to allow the diffusion of large permeant ions and of chlorpromazine through the upper part of the channel which is crowded by bulky side-chains (see sequences), the helices must be tilted away from the central axis by about 7° [6]. Two other crucial features of the model are, on

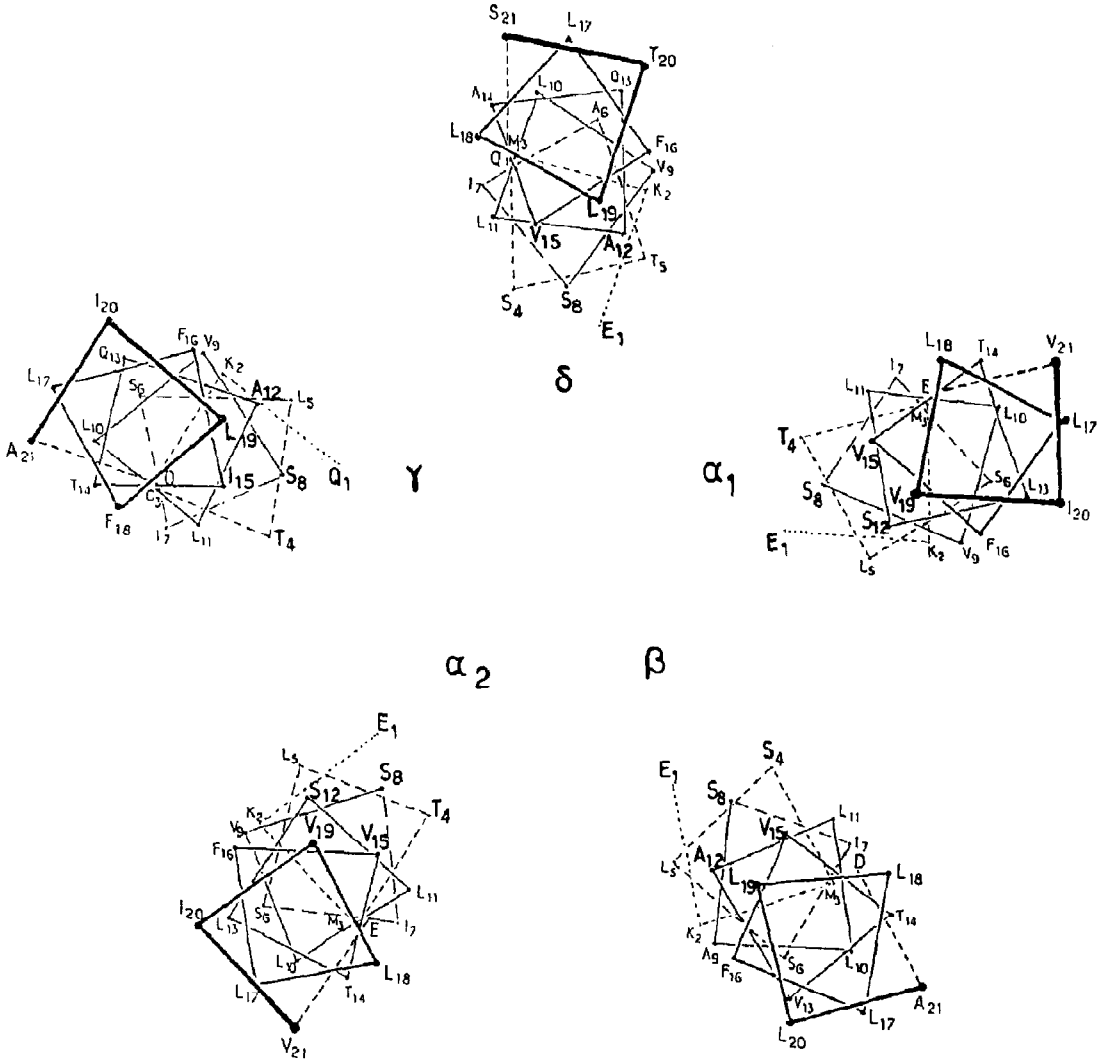

Fig. 2. Perspective view, from the synaptic side, of the disposition of the C_α carbons of the five MII helices surrounding the pore in the model of the channel. Bold-face characters are used for the amino acids which line the channel inner wall. Numbering as in fig. 1.

the one hand, the assumption that the charged glutamates (Gln in γ) and the adjacent lysines situated at the N-terminal of the MII segments belong to the α-helical structure and, on the other, the observation [6,7] that on the C-terminal side the α-helical stretch must be interrupted one residue before the charged residues, owing to the presence of a proline four residues above (see fig. 1). Calculations of the energy profile of the largest permeant ion dimethyldiethanolammonium (DMDEA) showed that the first assumption is decisive in determining the possibility of exit of the ions [5], a feature resulting from the α-helical structure which, together with the internal positions of the labelled serines, implies that the negatively charged glutamates (Gln in γ) also face the interior of the pore while the adjacent positively charged lysines point to the external side of the helices, and thus do not annihilate the favorable action of the negative residues. These conclusions, and hence the underlying hypothesis, have been strikingly confirmed by site-directed mutation experiments [9] which showed that mutating the negatively charged residues situated at the N-terminal has a much stronger effect on the channel conductance than mutating the other anionic residues found between MI and MII or between MII and MIII, while mutating the positively charged residues following the N-terminal Glu (Gln in γ) positions leads to no significant change in channel conductance. The smaller effect of the negative residues at positions 22 with respect to that of the residues at position 1 (see fig. 1) confirms the hypothesis that the upper ones are outside the limits of the α-helices in our model. Calculations [7] of energy profiles have, furthermore, indicated the role of the three other helices of each subunit and shown that their effect on the profiles could be mimicked by supplementing the cone of MIIs by another cone (rotated, with respect to the inner one, by 72° around the central vertical axis of the pore) of appropriate α-helices antiparallel to the first ones and placed in contact with them just behind in such a way that each of these helices is at an equal distance from two adjacent MIIs.

The availability of a model at the atomic level provides coordinates enabling the calculation of the energy profiles felt by an ion upon crossing the channel. We present below such calculations performed respectively in the wild-type and in characteristic mutants of ref. 9 in view of examining whether they correlate with the evolution of the conductances observed experimentally. Furthermore, since such profiles are a way to 'probe' the field felt by the cation at all levels in the interior of the channel, we exploit them to follow the effect of the different residues.

2. Methodological details

The calculation of the energy profile is performed as described in detail earlier [5–7,10,11] by optimization of the energy of interaction [12] of the ion with the whole channel in successive planes perpendicular to the central axis, regularly and closely spaced. The 'energy profile' is given as the plot of this interaction energy as a function of the progression of the ion. The helices in the model channel are maintained fixed, i.e., all intermolecular variables are frozen, but the side-chains of residues 4, 12, 15 and 19 (see fig. 2) are allowed complete freedom during the passage of the ion. Although a first exploration of energy profiles can be carried out in a frozen structure (see refs 7 and 13), allowance for the flexibility of the internal side-chains is important in the present case where the lower half of the channel contains flexible polar residues, particularly serines (positions 12, 8 and 4), which can use the lability of their side-chain to turn at best their attractive oxygen towards the cation [14] along its path. The threonines (in positions 4 in α and γ, and 5 in δ), although less flexible than the serines owing to the hindering presence of the methyl group, can nevertheless use their hydroxyl oxygen similarly, albeit in a less optimal way (vide infra). As a result of the introduction of the flexibility of the internal residues, a general lowering of the profiles occurs with a deepening and more accurate location of the energy minima, as well as a lowering of the spurious barriers [14]. For convenience and consistency with our previous work [7,13,14], the calculations have been performed for a sodium cation.

The mutations considered are those involving the N-terminal glutamates, mutated into gluta-

mines in α, β and δ (denoted αEQ, βEQ and δEQ, respectively) and into aspartate in α (αED). The introduction of the mutations is made as follows: according to energy optimizations carried out in our model of the wild type [5–7] Glu 1 and Lys 2 form a salt bridge in α, β, δ; Gln 1 and Lys 2 in γ form an H-bond. In keeping with this last result, whenever a glutamine was substituted to a glutamate in a mutant as in αEQ, βEQ, δEQ, it was allowed to form a hydrogen bond with its adjacent lysine as in MIIγ of the wild type. For the αED mutant, energy optimization showed that the aspartate and lysine side chains can still form a strong salt-bridge despite the shorter length of the Asp side-chain. The non-mutated residues are kept in the conformations of the wild type except for those lining the inner wall.

3. Results and discussion

The energy profiles obtained in the manner described above are given in fig. 3. To illustrate the correlation with the conductance data, points corresponding to the inward conductance observed in ref. 9 for each mutant are plotted on a conductance scale on the right. Table 1 lists for each energy well in the profiles the atoms involved in the strongest interactions with the ion.

The general overall characteristics of the profiles are similar in all mutations, all comprising five well-defined energy wells separated by barriers of different heights. The loci of the wells and barriers tops are essentially the same along the height of the channel in each energy profile. However, some displacements are observed in the case of βEQ and αEQ, a reflection of the different weights of the different side-chains in the interaction with the ion at the same height in different mutants (table 1) with a non-negligible effect on the conductance (vide infra).

In the first part of the profiles, down to the third minimum, the energy curves remain essentially parallel, undergoing only an upward displacement clearly due to the suppression of the

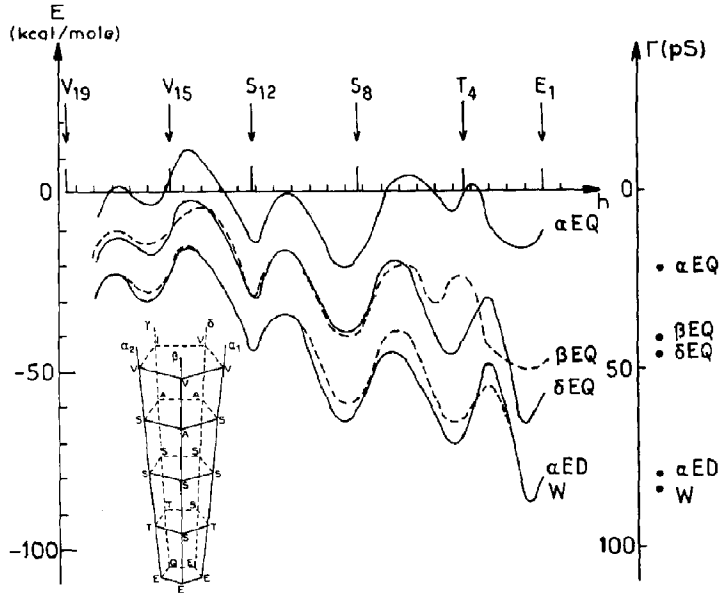

Fig. 3. Energy profiles computed for Na^+ in the model channel. W, δEQ and αEQ in unbroken lines; αED and βEQ in broken lines. The scale h indicates the height of the ion within the channel (path from synaptic side, left, to cytoplasmic side, right). The arrows indicate the height of the carbonyl oxygen atom of the residues facing the interior of the pore in MIIα of the wild type (see inset for homologs). Right scale: inward conductances measured for K^+ in ref. 9. The inset gives a schematic reminder of the composition of the inner wall for each helix in W.

Table 1

Residues (see fig. 2) and atoms (a) involved in the strongest interactions between Na^+ and the MIIs in the model channel for the wild-type and the αED, δEQ, βEQ and αEQ mutants (α_1, α_2 as in fig. 2)

(b)	1	2	3	4	5
W	V_{15}, α_2, O′	S_{12}, α_1, O′ S_{12}, α_1, O_γ	S_{12}, α_1, O_γ S_8, α_1, O′ S_8, α_1, O_γ	S_8, β, O_γ S_4, β, O′ S_4, β, O_γ	S_4, β, O_γ E_1, α_1, O_ϵ
αED	V_{15}, α_2, O′	S_{12}, α_1, O′ S_{12}, α_1, O_γ	S_{12}, α_1, O_γ S_8, α_1, O′ S_8, α_1, O_γ	S_8, β, O_γ S_4, β, O′ S_4, β, O_γ	T_4, α_2, O_γ E_1, β, O_ϵ
δEQ	V_{15}, α_2, O′	S_{12}, α_1, O′ S_{12}, α_1, O_γ	S_{12}, α_1, O_γ S_8, α_1, O′ S_8, α_1, O_γ	S_8, β, O_γ S_4, β, O′ S_4, β, O_γ	T_4, α_2, O_γ E_1, β, O_ϵ
βEQ	V_{15}, α_2, O′	S_{12}, α_1, O′ S_{12}, α_1, O_γ	S_{12}, α_1, O_γ S_8, α_1, O′ S_8, α_1, O_γ	S_8, α_1, O_γ T_4, α_1, O′	T_4, α_1, O_γ T_5, δ, O_γ E_1, δ, O_ϵ
αEQ	V_{15}, α_2, O′	S_{12}, α_1, O′ S_{12}, α_1, O_γ	S_{12}, α_1, O_γ S_8, α_1, O′ S_8, α_1, O_γ	S_8, β, O_γ S_4, β, O′ S_4, β, O_γ	T_4, α_1, O_γ T_5, δ, O_γ E_1, δ, O_ϵ

(a) O′, peptide carbonyl oxygen; O_γ, hydroxyl oxygen of the Ser or Thr side-chain; O_ϵ, the oxygen of the Glu side-chain not involved in the salt bridge with Lys.
(b) Position of the well in the energy profile from left (synaptic side) to right (cytoplasmic side) (fig. 3).

long-range attraction of one (βEQ, δEQ), then two (αEQ), negatively charged residues at the bottom of the channel. This long-range effect is not sufficient to modify drastically the trajectory followed by the ion, as seen in the first three columns of table 1: the first three sites reached by the cation, at every height, are essentially the same for the wild type, W, and for all mutants in this portion of the channel. The first one involves the carbonyl oxygen of V_{15} on α_2 *, the second the carbonyl oxygen of S_{12} of α_1 together with its hydroxyl oxygen; this last atom accompanies the ion to the third site where its attraction is supplemented by that of the carbonyl and hydroxyl oxygens of S_8 on the same helix.

In the lower part of the channel, differential effects appear both in the height and location of the sites and in the trajectory of the ion. As concerns the fourth site, its location is the same in W and in all mutants except βEQ: in all cases except βEQ (table 1), it is produced by the converging attraction of the hydroxyl oxygen of S_8 on β and the carbonyl and hydroxyl oxygens of S_4 on β. In the βEQ energy profile the fourth minimum corresponds instead to a strong interaction of Na^+ with S_8 and T_4 of α_1. Due to the presence of T_4 in α instead of S_4 in β, this site is displaced by 1 Å towards the synaptic side. Moreover, the presence of the methyl group of Thr prevents the ion interacting at best simultaneously with all three available oxygens (O_γ of S_8, O′ of T_4 and O_γ of T_4) so that only two strong interactions are achieved resulting in a lesser depth of the well in the βEQ curve (see fig. 3).

Concerning the fifth minimum, let us consider W, αED and δEQ: in the wild type the strongest interaction is obtained when the ion is roughly equally distant (about 2 Å) from the hydroxyl oxygen of S_4 of β and the carboxyl oxygen of E_1 of α_1, a region where the conjunction of the attractive effect of the four glutamates present is maximum. When the glutamate of α is replaced by Asp in αED the site becomes less favorable and the strongest interaction is displaced towards a point equidistant (again about 2 Å) from the hydroxyl oxygen of T_4 of α_2 and the carboxyl

* A nearly equivalent energy involves O′ of V_{15} on α_1.

oxygen of E_1 of β. This location between α_2 and β remains preferential in δEQ when the Glu of δ is replaced by Gln.

As concerns the βEQ and αEQ mutants another modification occurs in the location and shape of the fifth minimum: when E is changed to Q in β the ion comes closer to δ and interacts strongly with both side-chains of T_4 of α_1 and E_1 of δ, at an equal distance from the two available oxygen atoms. However, the presence of a threonine at position 5 in δ (instead of a Leu in the other MIIs) which can turn its hydroxyl oxygen towards the pore, brings about additional favorable interaction. This is already felt by the cation 2 Å above the level of the fifth energy minimum, resulting in a removal of the barrier which exists in this region in the W, αED and δEQ profiles, and thus in a flattening of the βEQ curve at its right extremity.

In the αEQ mutant where two glutamates only are present, on β and δ, the relative distribution of the other residues around the central axis of the pore brings also the last binding site for the cation between α_1 and δ, and the essential features observed at the right extremity of the βEQ energy profile are repeated with a decreased attraction. Note the intervention of T_5 of δ in the fifth site for the last two mutants.

From the point of view of the energy, the average height of the profiles of fig. 3 appears to follow the order: W < ≃ αED < δEQ < βEQ < αEQ, in striking agreement with the order of the observed values of the conductance. An approximately inverse relationship was found in ref. 9 between channel conductance and the change in the total negative charge in the ring of glutamates considered here. The relative energy location of the calculated profiles confirms and defines this correlation: the structural analysis given above indicates that in the first part of the channel, the number of negatively charged residues appears more important than their location on the ring but, in the second part, differences appear between the effect of mutating δ or β which allow the discrimination between the corresponding conductances in spite of the identical global charge. Similarly, the relative energy location of the W and αED profiles, together with structural analysis, provides a possible explanation for the small variation which is observed in the corresponding conductances despite the fact that not only is the global charge identical in both channels but such is also the charge of each helix when passing from W to αED.

4. Concluding remarks

The correlation observed between the average location of the energy profiles and the results of the conductance experiments appears to provide confirmation of the essential structural hypothesis lying at the basis of our model and recalled in section 1, in particular the orientation of the faces of the helices with respect to the interior of the channel, the inclusion of the Glu(Gln)-Lys residues in the α-helices and, probably, their involvement in salt-bridges (and/or hydrogen bonds).

Aside from establishing the role of the location of the mutated charges around the ring, the probing of the channel inner wall by the cation demonstrates the role of the other structural elements in forming the 'sites' encountered by the cation: peptide carbonyl oxygens of the upper wall, hydroxyl oxygens of Ser 12, 8 and 4 or Thr 4 and 5.

The fact that the analysis allows a discrimination between the βEQ and δEQ mutations and even a subtle distinction between the wild type and the αED mutant is gratifying. The role suggested for the threonines present at the bottom of the channel is intriguing and deserves more thorough consideration. Clearly, the non-identity of the internal residues in the five helices is not an indifferent element in the conductance behavior. Further calculations allowing relaxation of the complete system should help in improving the profiles [11,14] and in determining further the role of the various residues. At present, the model, as it stands, and the various calculations carried out within it, seem to allow a clear rationalization of intrinsic global features of the channel inner wall. It is hoped that further experimental and theoretical investigations will help in the refinement of the model and lead to progress towards a better understanding of the structure-function relationship in the nicotinic ACh receptor.

References

1 J. Giraudat, M. Dennis, T. Heidmann, J.Y. Chang and J.P. Changeux, Proc. Natl. Acad. Sci. U.S.A. 83 (1986) 2719.
2 J.P. Changeux and F. Revah, Trends Neurosci. 10 (1987) 245.
3 F. Hucho, Eur. J. Biochem. 158 (1986) 211.
4 F. Hucho, W. Oberthur and F. Lottspeich, FEBS Lett. 205 (1986) 137.
5 S. Furois-Corbin and A. Pullman, in: Transport through membranes: Carriers, channels and pumps, eds A. Pullman, J. Jortner and B. Pullman (Kluwer, Dordrecht, 1988) p. 337.
6 S. Furois-Corbin and A. Pullman, Biochim. Biophys. Acta 984 (1989) 339.
7 S. Furois-Corbin and A. Pullman, FEBS Lett. 252 (1989) 63.
8 A. Pullman and S. Furois-Corbin, in: Sixth conversation: Biomolecular stereodynamics, structure and methods, eds R.H. Sarma and M. Sarma, vol. II (Adenine Press, New York, 1990) p. 295.
9 K. Imoto, C. Busch, B. Sakmann, M. Mishina, T. Konno, J. Nakai, H. Bujo, Y. Mori, K. Fukuda and S. Numa, Nature 335 (1988) 645.
10 C. Etchebest and A. Pullman, J. Biomol. Struct. Dyn. 3 (1986) 805.
11 S. Furois-Corbin and A. Pullman, Biochim. Biophys. Acta 860 (1986) 165.
12 R. Lavery, H. Sklenar, K. Zakrzewska and B. Pullman, J. Biomol. Struct. Dyn. 3 (1986) 989.
13 A. Pullman, S. Furois-Corbin and A.M. Andrade, in: Modelling of molecular structure and properties (Proc. 44th Int. Meet. Phys. Chem., ed. J.L. Rivail (Elsevier, Amsterdam, 1990) vol. 71, p. 527.
14 S. Furois-Corbin and A. Pullman, J. Biomol. Struct. Dyn. 4 (1987) 589.